Cancer Research

MiR-26a Inhibits Cell Growth and Tumorigenesis of Nasopharyngeal Carcinoma through Repression of EZH2

Juan Lu[1,2], Ming-Liang He[2,3,4], Lu Wang[1,2], Ying Chen[2], Xiong Liu[1], Qi Dong[2], Yang-Chao Chen[3], Ying Peng[5], Kai-Tai Yao[6], Hsiang-Fu Kung[2,4], and Xiang-Ping Li[1]

Abstract

Several microRNAs (miRNA) have been implicated in nasopharyngeal carcinoma (NPC), a highly invasive and metastatic cancer that is widely prevalent in southern China. In this study, we report that microRNA miR-26a is commonly downregulated in NPC specimens and NPC cell lines with important functional consequences. Ectopic expression of miR-26a dramatically suppressed cell proliferation and colony formation by inducing G_1-phase cell-cycle arrest. We found that miR-26a strongly reduced the expression of *EZH2* oncogene in NPC cells. Similar to the restoring miR-26 expression, EZH2 downregulation inhibited cell growth and cell-cycle progression, whereas EZH2 overexpression rescued the suppressive effect of miR-26a. Mechanistic investigations revealed that miR-26a suppressed the expression of c-myc, the cyclin D3 and E2, and the cyclin-dependent kinase CDK4 and CDK6 while enhancing the expression of CDK inhibitors $p14^{ARF}$ and $p21^{CIP1}$ in an EZH2-dependent manner. Interestingly, cyclin D2 was regulated by miR-26a but not by EZH2, revealing cyclin D2 as another direct yet mechanistically distinct target of miR-26a. In clinical specimens, EZH2 was widely overexpressed and its mRNA levels were inversely correlated with miR-26a expression. Taken together, our results indicate that miR-26a functions as a growth-suppressive miRNA in NPC, and that its suppressive effects are mediated chiefly by repressing EZH2 expression. *Cancer Res; 71(1); 225–33. ©2011 AACR.*

Introduction

Nasopharyngeal carcinoma (NPC) is a squamous cell carcinoma derived from epithelial cells located in the nasopharynx, which is highly malignant with local invasion and early distant metastasis. Three major etiologic factors of NPC include genetic susceptibility, environmental factors, and Epstein–Barr virus (EBV) infection, but the molecular mechanism of its pathogenesis is not yet fully understood. A unique feature of NPC is that it has a remarkably unusual ethnic and geographic distribution in southern China and Southeast Asia, especially in individuals of Cantonese origin. In endemic regions, such as southern China, incidence of NPC has remained very high, with a 5-year overall survival rate of approximately 70% (1). Although excellent local control can be achieved with advances in radiation therapy, 30% to 40% of patients will develop distant metastasis within 4 years (2). Once metastasis occurs, the prognosis is very poor. Therefore, better understanding of the pathogenesis is essential for the development of novel effective therapies for NPC.

MicroRNAs (miRNA) are a diverse class of small, non–protein-coding RNAs that function as critical gene regulators. Bioinformatic analyses indicate that each miRNA regulates hundreds of target genes, underscoring the potential influences of miRNAs on almost every biological pathway (3, 4). Recent evidence has shown that about half of the human miRNAs are located in cancer-associated genomic regions and can function as tumor suppressor genes or oncogenes depending on their targets (5–7). To date, several human and EBV-encoded miRNAs have been shown to be dysregulated in NPC, such as miR-29c, miR-200a, miR-100, miR-141, miR-BART22, and miR-BART5 (8–13), which contribute to the development and progression of NPC. These findings suggest the involvement of miRNAs in NPC tumorigenesis. A recent study has shown that miR-26a is downregulated in NPC tissues compared with adjacent normal tissues by miRNA microarray analysis (14). However, the role of miR-26a in cancer cells seemed controversial as it served as an oncogene in glioma but

Authors' Affiliations: [1]Department of Otolaryngology-Head and Neck Surgery, Nanfang Hospital, Southern Medical University, Guangzhou; [2]Stanley Ho Center for Emerging Infectious Diseases, [3]Department of Medicine and Therapeutics, and [4]Li Ka Shing Institute of Health Sciences, Faculty of Medicine, The Chinese University of Hong Kong, Hong Kong; [5]Department of Neurology, The Second Affiliated Hospital, Sun Yat-sen University; and [6]Cancer Research Institute, Key Lab for Transcriptomics and Proteomics of Human Fatal Diseases, Southern Medical University, Guangzhou, China

Note: Supplementary data for this article are available at Cancer Research Online (http://cancerres.aacrjournals.org/).

Corresponding Authors: Xiang-Ping Li, Department of Otolaryngology-Head and Neck Surgery, Nanfang Hospital, Southern Medical University, Guangzhou 510515, China. Phone: 86-20-61642001; Fax: 86-20-87703645. E-mail: lp133402@yahoo.com.cn; or Ming-Liang He, Stanley Ho Center for Emerging Infectious Diseases, The Chinese University of Hong Kong, Hong Kong, China. Phone: 852-37636096; Fax: 852-21458013. E-mail: mlhe7788@gmail.com

doi: 10.1158/0008-5472.CAN-10-1850

as a tumor suppressor in liver cancer (15, 16). Until now, no functional evidence of miR-26a in NPC has been documented.

In this study, we investigated the potential involvement of miR-26a in NPC. We examined the expression level of miR-26a in human NPC cells and tissues and tested its effects on cell growth, cell-cycle distribution, and colony formation. In addition, we also investigated a potential role of miR-26a on NPC tumorigenesis in a murine model. Finally, we explored the underlying mechanism of miR-26a functions in NPC. Our study will provide a better understanding of NPC pathogenesis.

Materials and Methods

Cell culture and miRNA transfection

An immortalized nasopharyngeal epithelial cell NP69 was cultured in Keratinocyte-SFM (Invitrogen) supplemented with bovine pituitary extract (BD Biosciences) as described previously (17). The human NPC cell lines 5-8F, 6-10B, CNE1, CNE2, C666-1, HONE1, and HNE-1 were cultured in RPMI-1640 (Invitrogen; refs. 18, 19). HEK 293T cells were cultured in Dulbecco's modified Eagle's medium (DMEM; Invitrogen). MiRNAs were transfected at a working concentration of 100 nmol/L using Lipofectamine 2000 reagent (Invitrogen). The miR-26a mimic, a nonspecific miR control, anti-miR26a, and a nonspecific antimiR control were all purchased from Dharmacon.

Clinical specimens

Primary NPC biopsy specimens and normal biopsies of the nasopharynx were obtained from Nanfang Hospital (Southern Medical University, Guangzhou, China). Both tumor and normal tissues were histologically confirmed by H&E (hematoxylin and eosin) staining. Informed consent was obtained from each patient, and the research protocols were approved by the Ethics Committee of Nanfang Hospital.

Vector construction and lentivirus production

A 187-bp DNA fragment corresponding to pre–miR-26a and the flanking sequence was amplified from human genomic DNA and then cloned into pLVTHM lentiviral vector (http://www.addgene.org/Didier_Trono). Another 2 lentiviral vectors for cDNA and shRNA delivery of EZH2 were described previously (20, 21). The production, purification, and titration of lentivirus were performed as described by Tiscornia and colleagues (22). The packaged lentiviruses were named LV-miR26a, LV-EZH2, and LV-shEZH2, respectively. The empty lentiviral vector LV-con was used as a control.

MTT assay and cell-cycle analysis

Cells were plated in 96-well plates at 2×10^3 per well in a final volume of 100 μL and transfected with miRNAs. After transfection, the cells were cultured for 24, 48, 72, and 96 hours. The effect of miR-26a on cell growth and viability was determined by MTT assay as described previously (23). For cell-cycle analysis, cells were plated in 6-well plates at 2×10^5 per well and transfected with miRNAs. At 48 hours posttransfection, the cell-cycle distribution was analyzed by propidium iodide (PI) staining and flow cytometry as described by Singh and colleagues (24).

Colony formation assay

Cells were infected with LV-miR26a to stably overexpress miR-26a. After 72 hours of transfection, the cells were plated in 6-well plates at 2×10^2 per well and grown for 2 weeks. After 2 weeks, the cells were washed twice with PBS, fixed with methanol/acetic acid (3:1, v/v), and stained with 0.5% crystal violet. The number of colonies was counted under the microscope (25).

RNA isolation, reverse transcription, and quantitative real-time PCR

Total RNA was extracted using Trizol reagent (Invitrogen). To quantitate miR-26a expression, total RNA was polyadenylated and reversely transcribed using NCode miRNA First-Strand cDNA Synthesis kit (Invitrogen). To measure the mRNA levels of EZH2 and cell-cycle regulators, total RNA was reversely transcribed using ImProm-II Reverse Transcription System (Promega). Quantitative real-time PCR (qPCR) was performed using SYBR Green PCR master mix (Applied Biosystems) on an ABI 7500HT System. The primers were listed in Supplementary Table S1. GAPDH or U6 snRNA was used as an endogenous control. All samples were normalized to internal controls and fold changes were calculated through relative quantification ($2^{-\Delta\Delta Ct}$; ref. 26).

Western blot analysis

Protein lysates were separated by 10% SDS-PAGE, and electrophoretically transferred to PVDF (polyvinylidene difluoride) membrane (Millipore). Then, the membrane was incubated with mouse monoclonal antibody against human EZH2 (Cell Signaling Technology) followed by HRP (horseradish peroxidase)-labeled goat-antimouse IgG (Santa Cruz Biotechnology) and detected by chemiluminescence. Glyceraldehyde-3-phosphate dehydrogenase (GAPDH) was used as a protein-loading control. The intensity of protein fragments was quantified with the Quantity One software (4.5.0 basic, Bio-Rad).

MiRNA target validation

A 264-bp fragment of EZH2 3′UTR (untranslated regions) was amplified by PCR and cloned downstream of the firefly luciferase gene in pGL3 vector (Promega). The vector was named wild-type (wt) 3′UTR. Site-directed mutagenesis of the miR-26a binding site in EZH2 3′UTR was performed using GeneTailor Site-Directed Mutagenesis System (Invitrogen) and named mutant (mt) 3′UTR. For reporter assays, wt or mt 3′UTR vector and the control vector pRL-CMV [(cytomegalovirus) coding for Renilla luciferase, Promega) were cotransfected. Luciferase activity was measured 36 hours after transfection using the Dual-Luciferase Reporter Assay System (Promega).

Tumor growth assay

Female BALB/c nude mice aged 4 to 5 weeks were purchased from Laboratory Animal Services Centre of the Chinese University of Hong Kong (CUHK). Animal handling and experimental procedures were approved by the Animal

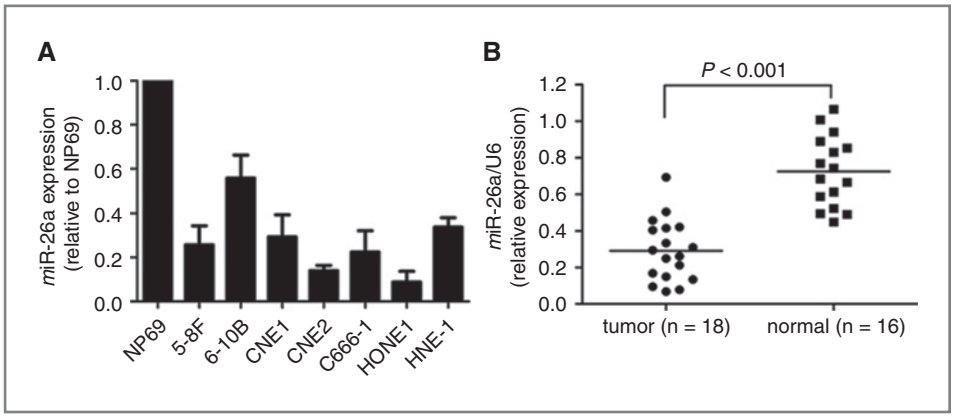

Figure 1. The expression of miR-26a was reduced in NPC cell lines and clinical specimens. A, expression of miR-26a in 7 NPC cell lines. B, average expression level of miR-26a in human NPC specimens ($n = 18$) and normal nasopharyngeal epithelial tissues ($n = 16$). miRNA abundance was normalized to U6 RNA.

Experimental Ethics Committee of CUHK. For tumor growth assay, C666-1 cells were infected with LV-miR26a [MOI (multiplicity of infection) = 100]. Following fluorescence-activated cell sorting, the green fluorescence protein (GFP)–positive cells were isolated and a total of 5×10^5 infected cells were injected subcutaneously into the dorsal flank of nude mice. Each group contained 5 mice and the experiment was repeated 3 times. Tumor size was measured every 2 days. When subcutaneous tumors reached the volume of 500 mm^3, mice were sacrificed and tumors were dissected. Tumor volumes were calculated as follows: volume = $(D \times d^2)/2$, where D meant the longest diameter and d meant the shortest diameter.

Immunohistochemistry

Formalin-fixed, paraffin-embedded tissues of transplanted tumors were sectioned at 4-μm thickness and analyzed for Ki-67 (Abcam; 1:50 dilution) and PCNA (proliferating cell nuclear antigen; Abcam, 1:1,000 dilution) expression. Visualization was achieved using the EnVision+ peroxidase system (Dako). A sample was considered positive if more than 50% of the tumor cells retained nuclear staining, and 5 fields were randomly selected according to semiquantitative scales (27). The intensity of staining was scored manually (high, 3; medium, 2; low, 1; no staining, 0) by 2 independent experienced pathologists, and only tumor cells were scored.

Statistical analysis

SPSS 13.0 software was used for statistical analysis. Data were presented as mean ± SEM of at least 3 independent experiments. Two-tailed Student's t test was used for comparisons of 2 independent groups. The relationship between EZH2 and miR-26a expression was explored by Spearman's correlation. Ki-67 and PCNA expression was analyzed by Mann–Whitney U test. P values of < 0.05 were considered statistically significant.

Results

MiR-26a was downregulated in human NPC cell lines and clinical specimens

A panel of human NPC cell lines was first analyzed to quantitate the expression level of miR-26a. The results showed that the expression level of miR-26a was decreased in all 7 NPC cell lines examined, compared with the immortalized nontumorigenic cell line NP69 (Fig. 1A).

We further examined the expression level of miR-26a in 18 NPC specimens and 16 normal nasopharyngeal epithelial tissues. Consistent with the data obtained from NPC cell lines, the average expression level of miR-26a was significantly lower in NPC specimens than in normal nasopharyngeal epithelial tissues (Fig. 1B; $P < 0.001$).

MiR-26a induced growth inhibition in NPC cells

To explore the effect of miR-26a on cell growth, C666-1 and HNE-1 cells were transiently transfected with miR-26a mimic or anti-miR26a, respectively. As shown in Fig. 2A, the results of MTT assay displayed that miR-26a inhibited cell growth in C666-1 cells by 42% ($P < 0.01$) and in HNE-1 cells by 55% ($P < 0.01$), whereas anti-miR26a promoted cell growth in C666-1 cells by 54% ($P < 0.01$) and in HNE-1 cells by 47% ($P < 0.01$). By contrast, the miR control or antimiR control had no effect on cell growth, indicating that the effect caused by miR-26a was highly specific.

Following observation of miR-26a–mediated growth inhibition, we transfected C666-1 cells with miR-26a mimic or antimiR-26a and examined cell-cycle distribution. Compared with miR control, C666-1 cells transfected with miR-26a displayed an increased percentage of cells in G_1 phase and fewer cells in S phase (Fig. 2B; $P < 0.01$), but the cell-cycle distribution had no significant difference between antimiR control and anti-miR26a–transfected cells. These results suggested that the growth-suppressive effect of miR-26a was partly due to a G_1-phase arrest.

We next used lentiviral vectors to stably restore the expression of miR-26a in C666-1 and HNE-1 cells and examined cell growth rate and cell-cycle distribution. We showed that the expression levels of miR-26a were increased in C666-1 and HNE-1 cells respectively in a dose-dependent manner and reached a very high level at MOI 100 (Fig. 2C). Therefore, the same condition (MOI = 100) was applied for further experiments. The growth inhibition induced by LV-miR26a infection was similar to that induced by miR-26a mimic transfection, and a G_1-phase arrest was also observed in LV-miR26a infected cells in a similar way (data not shown). As demon-

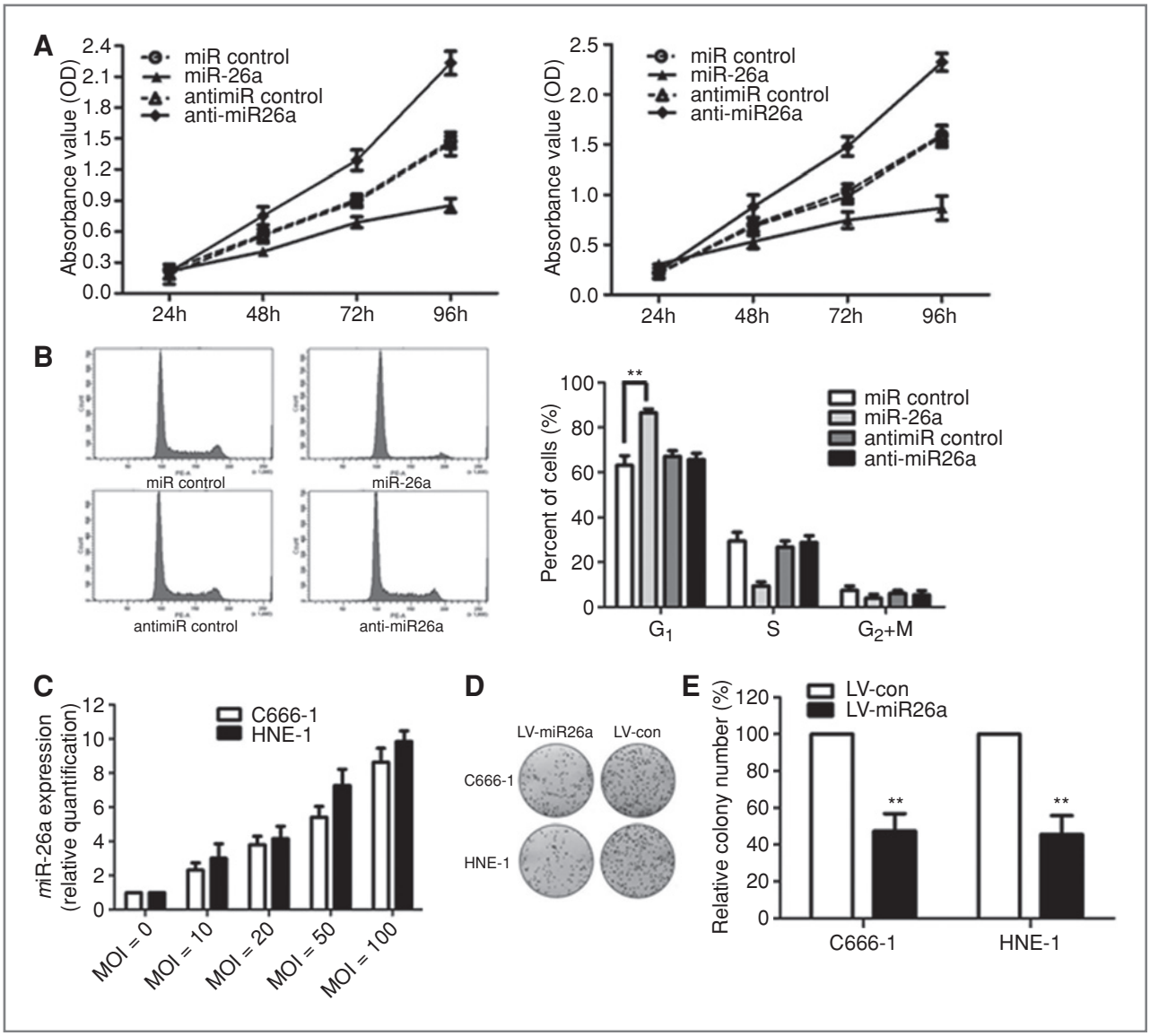

Figure 2. Enforced expression of miR-26a induced growth inhibition in NPC cells. A, effect of miR-26a on cell proliferation was measured by MTT assay after miRNA transfection in C666-1 and HNE-1 cells. B, representative histograms for cell-cycle distribution of C666-1 cells transfected with miRNAs for 48 hours. C, expression levels of miR-26a after C666-1 and HNE-1 cells were infected with LV-miR26a at 5 different MOIs. D, representative pictures of colony formation assay of LV-miR26a–infected C666-1 and HNE-1 cells. E, colonies were evaluated and values were reported as the ratio between LV-miR26a-infected cells and LV-con–infected cells. **, $P < 0.01$ compared with control.

strated in colony formation assay, LV-miR26a–infected C666-1 and HNE-1 cells displayed much fewer and smaller colonies compared with LV-con–infected cells (Fig. 2D and E; $P < 0.01$).

EZH2 was a direct target of miR-26a in NPC cells

To explore the mechanism of growth inhibition induced by miR-26a, we investigated whether miR-26a could regulate EZH2 expression in NPC cells. *EZH2*, a bona fide oncogene, was reported to be a target of miR-26a in some cells (28–30). However, the status and the function of EZH2 have never been studied in NPC. We transduced C666-1 and HNE-1 cells with LV-miR26a at 5 different MOIs of 0, 10, 20, 50, and 100 and then examined EZH2 expression levels. As shown in Fig. 3A, ectopic expression of miR-26a led to a dose-dependent decrease in EZH2 mRNA and protein levels. At MOI 100, both the mRNA and protein levels of EZH2 were decreased by approximately 70% to 80%. Moreover, inhibition of endogenous miR-26a by anti-miR26a resulted in upregulated expression of EZH2 in HNE-1 cells (Fig. 3B).

We further performed luciferase reporter assay to determine whether miR-26a could directly target the 3′UTR of EZH2 in NPC cells. The target sequence of EZH2 3′UTR (wt 3′UTR) or the mutant sequence (mt 3′UTR) was cloned into a luciferase reporter vector (Fig. 3C). C666-1 cells were then

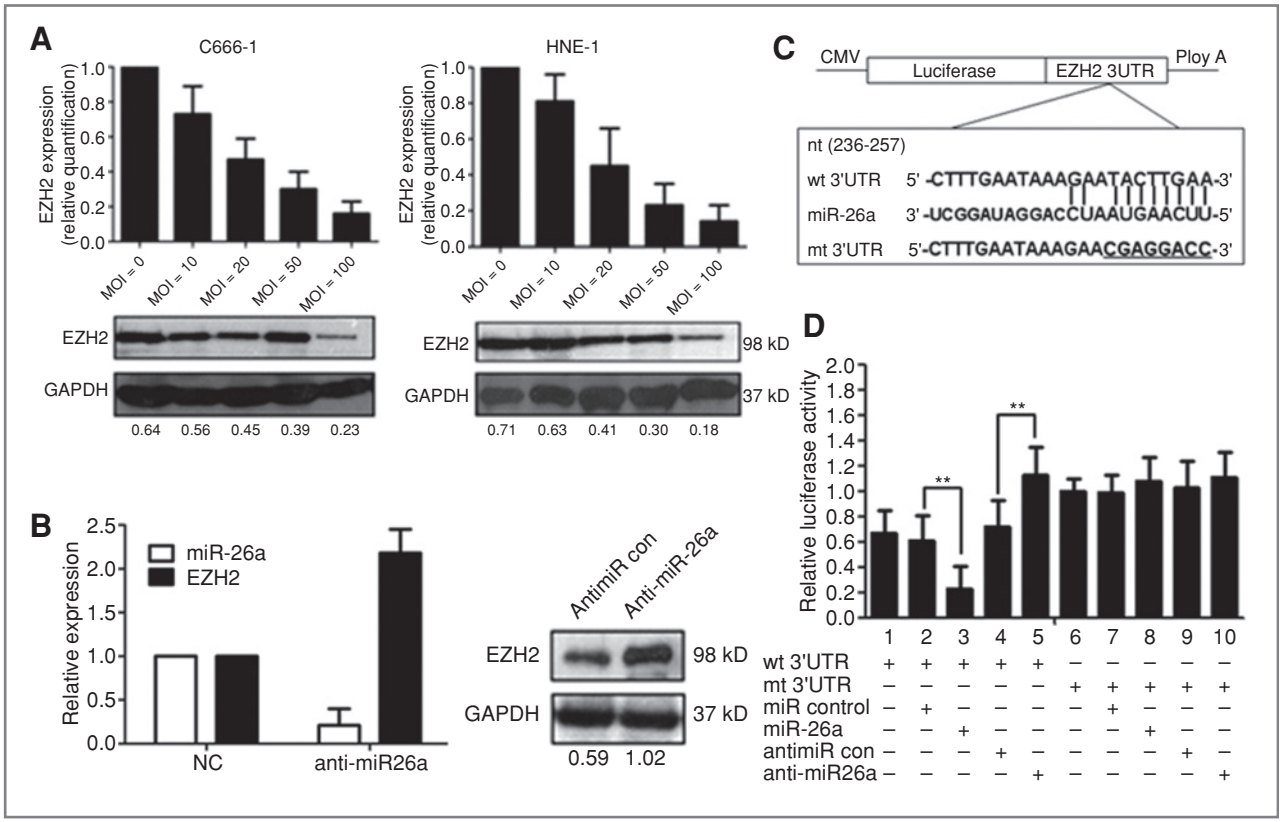

Figure 3. EZH2 was a direct target of miR-26a in NPC cells. A, expression levels of EZH2 after LV-miR26a infection at different MOIs in C666-1 and HNE-1 cells. B, expression levels of miR-26a and EZH2 after HNE-1 cells were transfected with anti-miR26a for 48 hours. C, diagram of EZH2 3′UTR–containing reporter constructs. D, luciferase reporter assays in C666-1 cells, with cotransfection of wt or mt 3′UTR and miRNAs as indicated. **, $P < 0.01$ compared with control.

transfected with wt or mt 3′UTR vector and miR-26a mimic. The results showed a significant decrease of luciferase activity when compared with miR control (Fig. 3D, lanes 2 and 3; $P < 0.01$). The activity of mt 3′UTR vector was unaffected by a simultaneous transfection with miR-26a (Fig. 3D, lanes 7 and 8). Moreover, cotransfection with anti-miR26a and wt 3′UTR vector in C666-1 cells led to a 2-fold increase of luciferase activity (Fig. 3D, lanes 4 and 5; $P < 0.01$). Taken together, all these results strongly suggested that EZH2 was a direct target of miR-26a in NPC cells.

To elucidate whether the growth-suppressive effect of miR-26a was mediated by repression of EZH2 in NPC cells, we performed gain-of-function and loss-of-function studies. First we silenced EZH2 to investigate whether the reduced expression of EZH2 could mimic the suppressive effect of miR-26a. C666-1 cells were infected with LV-shEZH2 or LV-miR26a and then we examined cell growth rate and cell-cycle distribution. As shown in Fig. 4A, EZH2 knockdown led to significant cell growth inhibition and cell-cycle arrest, similar to those induced by miR-26a ($P < 0.01$). Subsequently, we evaluated whether ectopic expression of EZH2 could rescue the suppressive effect of miR-26a. C666-1 cells were infected with LV-miR26a for 72 hours and followed by infection with LV-EZH2, which encoded the full-length coding sequence without the 3′UTR region. We showed that ectopic expression of EZH2 significantly rescued miR-26a–induced cell growth inhibition and cell-cycle arrest (Fig. 4B, $P < 0.01$).

Cell-cycle regulators contributed to the growth inhibition induced by miR-26a

The p53 and pRb pathways are involved in the regulation of cell-cycle progression and frequently deregulated in cancers. *c-myc* is one of the most important oncogenes which promote cell proliferation. To reveal whether these regulators were involved in the growth inhibition of miR-26a, we checked the mRNA levels of 14 cell-cycle regulators in C666-1 cells by qPCR including c-myc; cyclin D1 to D3 (CCND1, CCND2, CCND3); cyclin E1 and E2 (CCNE1, CCNE2); cyclin-dependent kinase 2, 4, and 6 (CDK2, CDK4, CDK6); and cell-cycle inhibitors $p14^{ARF}$, $p16^{INK4A}$, $p21^{CIP1}$, p53, and pRb. We demonstrated that the levels of CCND2, CCND3, CCNE2, CDK4, CDK6, and c-myc were decreased by more than 3-fold, whereas the levels of tumor suppressors, $p14^{ARF}$ and $p21^{CIP1}$, were increased at least 3.5-fold after miR-26a overexpression. By contrast, anti-miR26a treatment produced opposite results (Fig. 5A). To further elucidate whether these genes were directly regulated by miR-26a or indirectly by EZH2, we examined their

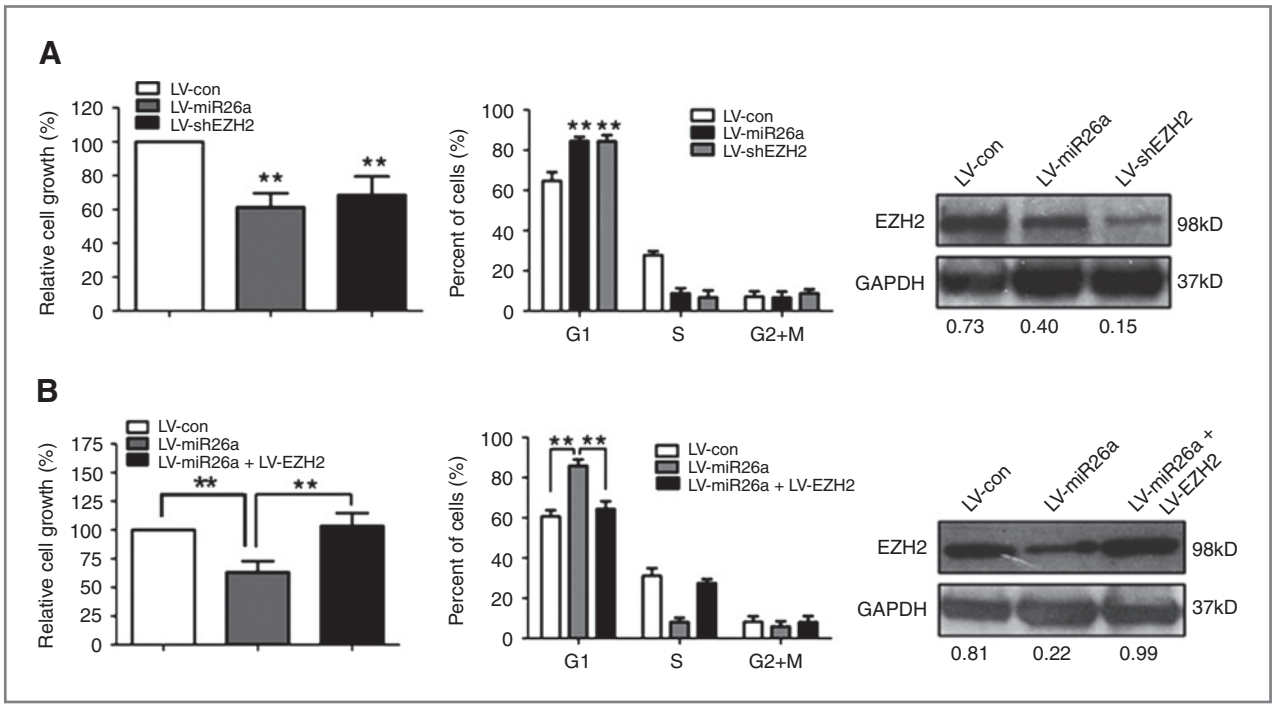

Figure 4. EZH2 was involved in miR-26a-induced growth inhibition in NPC cells. A, C666-1 cells were infected with LV-shEZH2 or LV-miR26a. Cell growth rate and cell-cycle distribution were measured by MTT assay and flow cytometry. B, C666-1 cells were infected with LV-miR26a for 72 hours, followed by infection with LV-EZH2, and MTT assay and cell-cycle analysis were then performed. **, $P < 0.01$ compared with control or comparison between 2 groups as indicated.

expression levels in LV-EZH2 or LV-shEZH2–infected C666-1 cells. For CCND3, CCNE2, CDK4, CDK6, c-myc, $p14^{ARF}$, and $p21^{CIP1}$, we found that the effects of EZH2 upregulation were consistent with those of miR-26a downregulation, and silence of EZH2 or ectopic expression of miR-26a yielded similar results (Fig. 5B). In addition, we showed that EZH2 overexpression rescued the expression of those miR-26a effectors (Fig. 5C). Interestingly, CCND2 was only regulated by miR-26a but did not respond to EZH2. A summary diagram that outlines this regulatory network is shown in Fig. 5D.

MiR-26a suppressed tumor growth of NPC cells in nude mice

C666-1 cells were infected with LV-miR26a and then were injected subcutaneously into the dorsal flank of nude mice. The tumor became palpable between 5 and 7 days after inoculation, and all the mice developed tumors at the end of the experiment (Fig. 6A). As early as 9 days postimplantation, the growth of transplanted tumors between 2 groups became statistically significant ($P = 0.018$). At 2 weeks after implantation, those mice injected with LV-con carried larger burdens. As compared with control, the average tumor volume of the LV-miR26a–treated group was markedly reduced by more than 65% (Fig. 6B and C; $P < 0.001$). The average tumor weight was also significantly reduced in the LV-miR26a–treated group (0.21 ± 0.11 g vs. 0.82 ± 0.21 g; $P < 0.01$), but no difference in body weight was found between the miR-26a–treated and the control mice (data not shown). We also showed that both the staining intensity and the number of hyperproliferative Ki-67^+ and $PCNA^+$ tumor cells were significantly decreased compared with control (Fig. 6D and Supplementary Table S2; $P < 0.05$).

EZH2 was upregulated in NPC specimens and inversely correlated with miR-26a levels

We further measured the mRNA levels of EZH2 in NPC specimens and normal nasopharyngeal epithelial tissues. The results showed that the average expression level of EZH2 was significantly higher in NPC specimens than in normal nasopharyngeal tissues (Fig. 7A; $P < 0.01$). Then, we correlated EZH2 with miR-26a expression in the same NPC specimens. As shown in Fig. 7B, when EZH2 mRNA levels were plotted against miR-26a expression, a significant inverse correlation was observed (2-tailed Spearman's correlation, $r = -0.831$; $P < 0.001$).

Discussion

NPC is a unique head and neck cancer because of its unusual ethnic association, geographic distribution, and consistent association with latent EBV infection. A preliminary study has shown that miR-26a was downregulated in NPC tissues (14), but no data are available about its functions. Our results also displayed the decreased expression of miR-26a in 7 NPC cell lines and NPC tissues (Fig. 1). We selected the undifferentiated C666-1 and HNE-1 cells, which exhibited

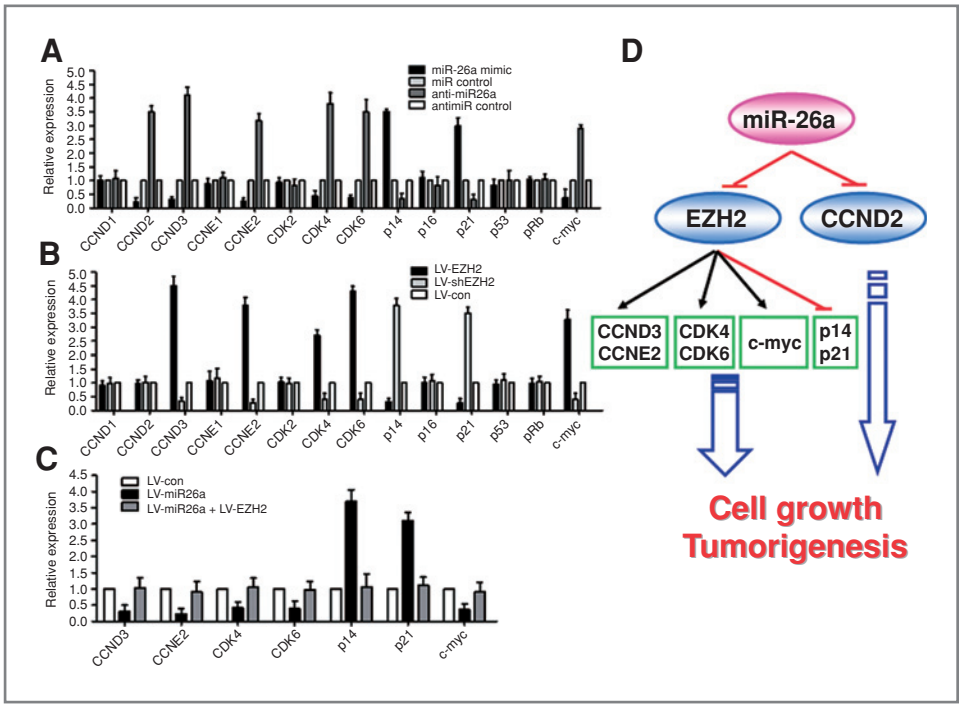

Figure 5. Cell-cycle regulators contributed to the growth inhibition induced by miR-26a. A, deregulated expression of 14 cell-cycle regulators in C666-1 cells after miR-26a mimic or inhibitor transfection. B, their dysregulated expression in C666-1 cells after LV-EZH2 or LV-shEZH2 infection. C, EZH2 overexpression rescued the deregulated expression of miR-26a effectors in C666-1 cells. D, a diagram of miR-26a signaling pathways for cell-cycle control in NPC cells.

similar clinical phenotypes of NPC, as the most suitable model for further experiments.

To reveal the role of miR-26a in NPC cells, we tested the effect of miR-26a on cell growth. Our results showed that miR-26a could inhibit cell growth and colony formation, induce a G_1 arrest in NPC cells (Fig. 2), and suppress tumorigenesis in a murine model of NPC xenograft (Fig. 6), suggesting its potential tumor suppressor role in NPC. The data were similar to the findings in liver cancer and lymphoma, in which miR-26a was downregulated, and ectopic expression of miR-26a suppressed cell proliferation and induced a G_1-phase arrest (16, 30, 31). However, miR-26a was amplified and could promote cell growth in glioblastoma and glioma (15, 32). These controversial results suggested that the role of miR-26a was possibly tumor specific and highly dependent on its targets in different cancer cells. Indeed, the tissue- and time-dependent expression of miRNAs influenced protein translation during distinct cellular processes, and the aberrant expression of their target genes affected different biological pathways with diverse functions (3).

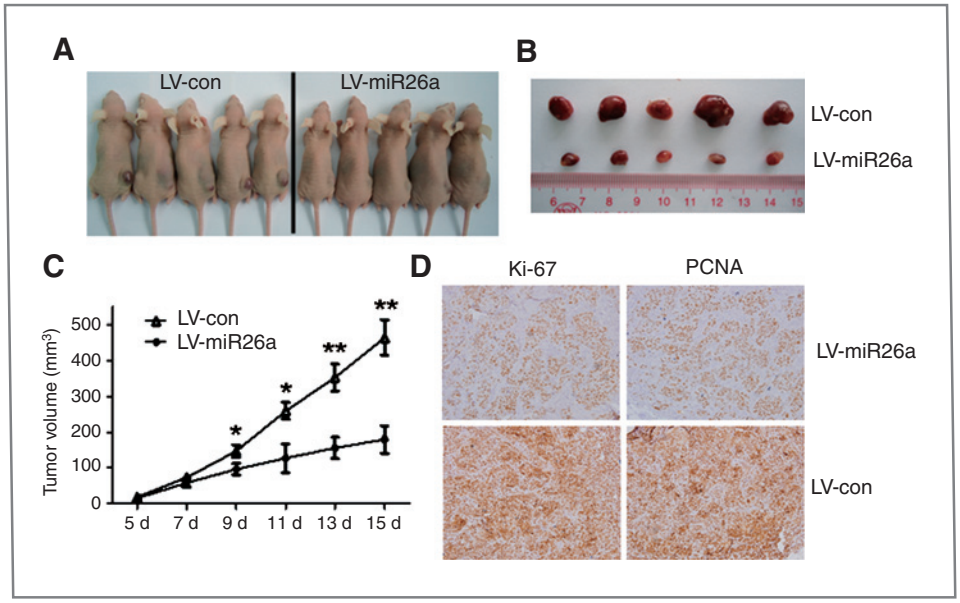

Figure 6. MiR-26a suppressed tumor growth of NPC cells in nude mice. A, C666-1 cells were infected with LV-miR26a and injected subcutaneously into nude mice. At 2 weeks after implantation, LV-miR26a-infected cells produced smaller tumors than control cells. B, representative picture of tumors formed. C, growth curve of tumor volumes. Each data point represents the mean ± SEM of 5 mice. D, Ki-67- and PCNA-stained sections of transplanted tumors formed by C666-1 cells infected with LV-miR26a at 2 weeks after orthotopic transplantation. Magnification, 200×. *, $P < 0.05$; **, $P < 0.01$ compared with control.

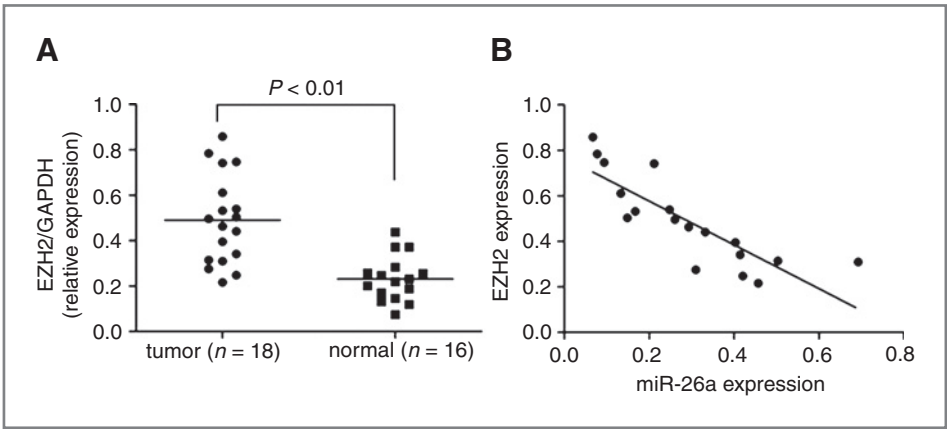

Figure 7. EZH2 was upregulated in NPC specimens and inversely correlated with miR-26a levels. A, average expression level of EZH2 in human NPC specimens and normal nasopharyngeal tissues. EZH2 abundance was normalized to GAPDH. B, a statistically significant inverse correlation between miR-26a and EZH2 mRNA levels in NPC specimens (Spearman's correlation analysis, $r = -0.831$; $P < 0.001$).

EZH2 belongs to the family of Polycomb group (PcG) proteins and plays a master regulatory role in many important cellular processes (33). Mounting evidence has shown that EZH2 is overexpressed in multiple cancers and can enhance cell proliferation and neoplastic transformation (34–37). However, the status and function of EZH2 have never been documented in NPC. Previous studies have identified EZH2 as a target of miR-26a in rhabdomyosarcoma and lymphoma (29, 30). In our studies, we demonstrated that miR-26a inhibited EZH2 expression in a dose-dependent manner, and confirmed that EZH2 was a direct target of miR-26a in NPC cells (Fig. 3). To further reveal the functions of EZH2 in NPC, we found that knockdown of EZH2 induced cell growth inhibition and a G_1-phase arrest similar to the phenotypes induced by miR-26a restoration, and EZH2 overexpression could rescue the growth-suppressive effect of miR-26a (Fig. 4). These results suggested that the growth inhibitory effect of miR-26a was partly mediated by repressing EZH2 expression.

It is well known that an average miRNA has approximately 100 target sites and regulates a large fraction of protein-coding genes, which form a regulatory network (38). To further explore the molecular mechanisms of growth inhibition induced by miR-26a, we examined the expression of a panel of cell-cycle regulators on p53 and pRb pathways. These genes included members of cyclins, CDKs, and CDK inhibitors as well as c-myc, which was devoted to the G_1–S transition. Our results demonstrated that the expression of CCND3, CCNE2, CDK4, CDK6, $p14^{ARF}$, $p21^{CIP1}$, and c-myc was indirectly regulated by miR-26a dependent on EZH2 (Fig. 5A and B). More importantly, we found that these deregulated expressions of miR-26a effectors could be restored by overexpression of EZH2 (Fig. 5C). Interestingly, independent of EZH2, CCND2 was directly regulated by miR-26a, indicating that it was a direct target of miR-26a in NPC cells, consistent with the data of Kota and colleagues in liver cancer (16). All these results documented that miR-26a repressed EZH2 expression, which, in turn, by mediating G_1-S checkpoint regulators, inhibited the growth and tumorigenicity of NPC cells. Our results also indicated that CCND1, CCNE1, CDK2, $p16^{INK4A}$, p53, and pRb were not the targets of either miR-26a or EZH2 (Fig. 5A and B). As summarized in Fig. 5D, EZH2 is likely the main target of miR-26a for the inhibitory effects on NPC cell growth.

In addition to the oncogenic effects of *EZH2* in NPC cells, for the first time, we showed that EZH2 was naturally upregulated in NPC specimens and inversely correlated with miR-26a levels (Fig. 7), suggesting that EZH2 might play important roles in NPC tumorigenesis. We suggested that the overexpression of EZH2 in NPC held significant promise for the advancement of cancer therapy, either in terms of improving diagnosis or predicting prognosis. Although this claim awaited further validation on larger sizes of samples, EZH2-dysregulated levels might prove valuable as prognostic markers, especially as EZH2 overexpression seemed to be strongly associated with the poor prognosis in both metastatic breast and prostate cancers (34, 37).

Taken together, this study identified miR-26a as a growth-suppressive miRNA in human NPC, at least, partly through repression of EZH2. Our data provide further evidence of a pivotal role of miRNAs in NPC tumorigenesis. As miR-26a is downregulated in NPC, reintroduction of this mature miRNA into the tumor tissue could provide a therapeutic strategy by reducing the expression of target genes. Although miRNA-based therapeutics are still in their infancy, our findings on miR-26a are encouraging and suggest that this miRNA could be a potential target for the treatment of NPC in future.

Disclosure of Potential Conflicts of Interest

This should be "No potential conflicts of interest were disclosed".

Grant Support

This work was supported by National Natural Science Foundation of China (grant no. 30772469, to X.-P. Li) and Research Grant Council of Hong Kong Government (CUHK4428/06M, to M.-L. He).

The costs of publication of this article were defrayed in part by the payment of page charges. This article must therefore be hereby marked *advertisement* in accordance with 18 U.S.C. Section 1734 solely to indicate this fact.

Received May 23, 2010; revised September 30, 2010; accepted October 26, 2010; published online January 3, 2011.

References

1. Lee AW, Yau TK, Wong DH, Chan EW, Yeung RM, Ng WT, et al. Treatment of stage IV(A-B) nasopharyngeal carcinoma by induction-concurrent chemoradiotherapy and accelerated fractionation. Int J Radiat Oncol Biol Phys 2005;63:1331–8.
2. Le QT, Tate D, Koong A, Gibbs IC, Chang SD, Adler JR, et al. Improved local control with stereotactic radiosurgical boost in patients with nasopharyngeal carcinoma. Int J Radiat Oncol Biol Phys 2003;56: 1046–54.
3. Ambros V. The functions of animal microRNAs. Nature 2004;431: 350–5.
4. Bartel DP. MicroRNAs: genomics, biogenesis, mechanism and function. Cell 2004;116:281–97.
5. Calin GA, Sevignani C, Dumitru CD, Hyslop T, Noch E, Yendamuri S, et al. Human microRNA genes are frequently located at fragile sites and genomic regions involved in cancers. Proc Natl Acad Sci U S A 2004;101:2999–3004.
6. Calin GA, Croce CM. MicroRNA signatures in human cancers. Nat Rev Cancer 2006;6:857–66.
7. Esquela-Kerscher A, Slack FJ. Oncomirs—microRNAs with a role in cancer. Nat Rev Cancer 2006;6:259–69.
8. Sengupta S, den Boon JA, Chen IH, Newton MA, Stanhope SA, Cheng YJ, et al. MicroRNA 29c is down-regulated in nasopharyngeal carcinomas, up-regulating mRNAs encoding extracellular matrix proteins. Proc Natl Acad Sci U S A 2008;105:5874–8.
9. Xia H, Ng SS, Jiang S, Cheung WK, Sze J, Bian XW, et al. miR-200a-mediated downregulation of ZEB2 and CTNNB1 differentially inhibits nasopharyngeal carcinoma cell growth, migration and invasion. Biochem Biophys Res Commun 2010;391:535–41.
10. Shi W, Alajez NM, Bastianutto C, Hui AB, Mocanu JD, Ito E, et al. Significance of Plk1 regulation by miR-100 in human nasopharyngeal cancer. Int J Cancer 2010;126:2036–48.
11. Zhang L, Deng T, Li X, Liu H, Zhou H, Ma J, et al. MicroRNA-141 is involved in a nasopharyngeal carcinoma-related genes network. Carcinogenesis 2010;31:559–66.
12. Lung RW, Tong JH, Sung YM, Leung PS, Ng DC, Chau SL, et al. Modulation of LMP2A expression by a newly identified Epstein-Barr virus-encoded microRNA miR-BART22. Neoplasia 2009;11:1174–84.
13. Choy EY, Siu KL, Kok KH, Lung RW, Tsang CM, To KF, et al. An Epstein-Barr virus-encoded microRNA targets PUMA to promote host cell survival. J Exp Med 2008;205:2551–60.
14. Chen HC, Chen GH, Chen YH, Liao WL, Liu CY, Chang KP, et al. MicroRNA deregulation and pathway alterations in nasopharyngeal carcinoma. Br J Cancer 2009;100:1002–11.
15. Huse JT, Brennan C, Hambardzumyan D, Wee B, Pena J, Rouhanifard SH, et al. The PTEN-regulating microRNA miR-26a is amplified in high-grade glioma and facilitates gliomagenesis *in vivo*. Genes Dev 2009;23:1327–37.
16. Kota J, Chivukula RR, O'Donnell KA, Wentzel EA, Montgomery CL, Hwang HW, et al. Therapeutic microRNA delivery suppresses tumorigenesis in a murine liver cancer model. Cell 2009;137:1005–17.
17. Tsao SW, Wang X, Liu Y, Cheung YC, Feng H, Zheng Z, et al. Establishment of two immortalized nasopharyngeal epithelial cell lines using SV40 large T and HPV16E6/E7 viral oncogenes. Biochim Biophys Acta 2002;1590:150–8.
18. Lung HL, Cheung AK, Xie D, Cheng Y, Kwong FM, Murakami Y, et al. TSLC1 is a tumor suppressor gene associated with metastasis in nasopharyngeal carcinoma. Cancer Res 2006;66:9385–92.
19. Song LB, Zeng MS, Liao WT, Zhang L, Mo HY, Liu WL, et al. Bmi-1 is a novel molecular marker of nasopharyngeal carcinoma progression and immortalizes primary human nasopharyngeal epithelial cells. Cancer Res 2006;66:6225–32.
20. Chen Y, Lin MC, Wang H, Chan CY, Jiang L, Ngai SM, et al. Proteomic analysis of EZH2 downstream target proteins in hepatocellular carcinoma. Proteomics 2007;7:3097–104.
21. Chen Y, Lin MC, Yao H, Wang H, Zhang AQ, Yu J, et al. Lentivirus-mediated RNA interference targeting enhancer of zeste homolog 2 inhibits hepatocellular carcinoma growth through down-regulation of stathmin. Hepatology 2007;46:200–8.
22. Tiscornia G, Singer O, Verma IM. Production and purification of lentiviral vectors. Nat Protoc 2006;1:241–5.
23. Tsang WP, Kwok TT. The miR-18a* microRNA functions as a potential tumor suppressor by targeting on K-Ras. Carcinogenesis 2009; 30:953–9.
24. Singh SV, Herman-Antosiewicz A, Singh AV, Lew KL, Srivastava SK, Kamath R, et al. Sulforaphane-induced G2/M phase cell cycle arrest involves checkpoint kinase 2-mediated phosphorylation of cell division cycle 25C. J Biol Chem 2004;279:25813–22.
25. Franken NA, Rodermond HM, Stap J, Haveman J, van Bree C. Clonogenic assay of cells *in vitro*. Nat Protoc 2006;1:2315–9.
26. Livak KJ, Schmittgen TD. Analysis of relative gene expression data using real-time quantitative PCR and the 2(-Delta Delta C(T)) Method. Methods 2001;25:402–8.
27. Efferson CL, Winkelmann CT, Ware C, Sullivan T, Giampaoli S, Tammam J, et al. Downregulation of Notch pathway by a gamma-secretase inhibitor attenuates AKT/mammalian target of rapamycin signaling and glucose uptake in an ERBB2 transgenic breast cancer model. Cancer Res 2010;70:2476–84.
28. Wong CF, Tellam RL. MicroRNA-26a targets the histone methyltransferase Enhancer of Zeste homolog 2 during myogenesis. J Biol Chem 2008;283:9836–43.
29. Ciarapica R, Russo G, Verginelli F, Raimondi L, Donfrancesco A, Rota R, et al. Deregulated expression of miR-26a and Ezh2 in rhabdomyosarcoma. Cell Cycle 2009;8:172–5.
30. Sander S, Bullinger L, Klapproth K, Fiedler K, Kestler HA, Barth TF, et al. MYC stimulates EZH2 expression by repression of its negative regulator miR-26a. Blood 2008;112:4202–12.
31. Ji J, Shi J, Budhu A, Yu Z, Forgues M, Roessler S, et al. MicroRNA expression, survival, and response to interferon in liver cancer. N Engl J Med 2009;361:1437–47.
32. Kim H, Huang W, Jiang X, Pennicooke B, Park PJ, Johnson MD. Integrative genome analysis reveals an oncomir/oncogene cluster regulating glioblastoma survivorship. Proc Natl Acad Sci U S A 2010;107:2183–8.
33. Sparmann A, van Lohuizen M. Polycomb silencers control cell fate, development and cancer. Nat Rev Cancer 2006;6:846–56.
34. Varambally S, Dhanasekaran SM, Zhou M, Barrette TR, Kumar-Sinha C, Sanda MG, et al. The polycomb group protein EZH2 is involved in progression of prostate cancer. Nature 2002;419:624–9.
35. Richter GH, Plehm S, Fasan A, Rössler S, Unland R, Bennani-Baiti IM, et al. EZH2 is a mediator of EWS/FLI1 driven tumor growth and metastasis blocking endothelial and neuro-ectodermal differentiation. Proc Natl Acad Sci U S A 2009;106:5324–9.
36. Croonquist PA, Van Ness B. The polycomb group protein enhancer of zeste homolog 2 (EZH2) is an oncogene that influences myeloma cell growth and the mutant ras phenotype. Oncogene 2005; 24:6269–80.
37. Kleer CG, Cao Q, Varambally S, Shen R, Ota I, Tomlins SA, et al. EZH2 is a marker of aggressive breast cancer and promotes neoplastic transformation of breast epithelial cells. Proc Natl Acad Sci U S A 2003;100:11606–11.
38. Brennecke J, Stark A, Russell RB, Cohen SM. Principles of microRNA-target recognition. PLoS Biol 2005;3:e85.